Electric Power Systems Research xxx (2016) xxx–xxx

Contents lists available at ScienceDirect

Electric Power Systems Research

journal homepage: www.elsevier.com/locate/epsr

Voltage support in industrial distribution systems in presence of induction generator-based wind turbines and large motors

M.A. Paez [a], M.B.C. Salles [a], C. Rahmann [b], A.P. Grilo [c,*]

[a] University of São Paulo, São Paulo, Brazil
[b] University of Chile, Santiago, Chile
[c] Universidade Federal do ABC, Brazil

ARTICLE INFO

Article history:
Received 4 January 2016
Received in revised form 28 April 2016
Accepted 1 May 2016
Available online xxx

Keywords:
Induction Generator
Large Motor Starting
Wind Power Generation

ABSTRACT

Industrial loads are usually composed of large induction motors (IM). These motors present a critical behavior under some circumstances, e.g. during starting and faults in the system. Currently, induction generator-based wind turbines are also connected to distribution systems. Essentially, these generators present the same behavior of large IM and, when directly connected to the system, their interaction can increase voltage sag levels or even lead the system to a voltage collapse. These generators, however, are usually provided with specific controls or power electronic-based equipment to comply with the voltage ride-through capability required by the grid codes. These resources, however, can be used to minimize the impact of large motors in the grid or even minimize their impact on voltage sags caused by faults in the system. In this context, this paper has the objective of analyzing the impact of different technologies used in induction generator-based wind turbines during disturbances in distribution systems in the presence of large IM. The analysis aims to clarify the potential benefit of wind turbine allocation at the demand side of an industrial power distribution system. Based on the results, an adapted control scheme, considering the control strategies currently available, is proposed for the grid side converter of the doubly fed induction generators to improve power quality.

1. Introduction

Among the different sources of power quality issues present in distribution system, the behavior of large Induction Motors (IM) represents an important one [1–3]. Basically, these motors produce or increase voltage sags during transitory operation conditions, which occurs during starting or voltage sags caused by faults in the system. In fact, the starting of large IM at distribution level may produce severe transients and voltage disturbances in the network, depending on their nominal power and operation cycle. The system can be affected not only locally but also in buses electrically remote from the motor connection point [4].

Currently, there are practical recommendations for industry and utilities [5,6] recommending the best practices for minimizing the problems caused by IM. However, these recommendations do not take into consideration that modern distribution networks have distributed generation, specially, wind turbines. Wind power has developed very fast and has achieved considerable penetration level compared to other kind of energy resources.

One of the most employed technologies for wind energy conversion is based on induction machines. Although these generators present the same behavior of large IM, the majority of them is provided with power electronic-based equipment, allowing some specific controls. Fundamentally, these controls have the objective of providing voltage support during disturbances in the grid, given the sensitive behavior of these machines.

The performance of power system considering either IM behavior [1–3,7] or operation control of wind turbines (WT)s [8–12] at distribution or subtransmission level has already been analyzed in several works. However, there are no studies about the dynamic interaction between WTs operation in industrial power distribution system with large IMs. The current literature covers the analysis of the operation of isolated systems equipped with WTs and IMs [2,13,14]. The operation of a distribution system with WTs and large IMs can be challenging during disturbances. During a voltage sag, the rotor speed of WTs based on induction generators will increase considerably, and the generator will need an additional amount of

Abbreviations: DFIG, Doubly Fed Induction Generator; LVRT, Low Voltage Ride-Through; IM, Induction Motor; GSC, Grid Side Converter; RSC, Rotor Side Converter; SCIG, Squirrel Cage Induction Generator; WT, Wind Turbine.

* Corresponding author.
E-mail address: ahda.pavani@ufabc.edu.br (A.P. Grilo).

http://dx.doi.org/10.1016/j.epsr.2016.05.001
0378-7796/

reactive power to sustain operation [9–11] (the characteristic of the rotor circuit become more inductive as the leakage reactance is proportional to the slip). At the same time, IM will also require more reactive power from the system due to the decrease in electromagnetic torque and reduction of the operation speed (increasing slip). Considering the aforementioned situation, the distribution system performance should be evaluated considering critical events in the system, such as motor starting and faults in the system.

This paper analyzes the use of voltage support capabilities available in induction generator-based wind turbines to minimize the impacts of large IM in distribution systems during the motor starting and system faults. As a consequence, the paper aims to clarify the potential benefit of wind turbine allocation at the demand side of an industrial power distribution system.

The analyses are based on simulations considering a typical distribution system with three large IM. Firstly, the interaction between a motor in operation and the starting process of a second and a third motor is investigated. Then, two types of WT generators are considered in the study: squirrel cage induction generator (SCIG) and doubly fed induction generator (DFIG). The DFIG-based WTs are the most installed worldwide, however, SCIG may still be found in some countries where wind power installations were carried out during the early stage or beginning of this technology development. In addition, a few manufactures, like Suzlon, were still commercializing the SCIG technology by 2012 [15].

As a result of these studies, it can be noticed, if the voltage support capability of wind turbines can reduce the impact of large IM on voltage sags. So, the different voltage support devices and control strategies are considered in the simulations. The selected cases are based on the existing technology and on possible advanced configurations that may need small changes in control algorithm only. For the SCIG, the options considered are: capacitor bank, Static Synchronous Compensator (STATCOM), and soft starter and STATCOM. For the DFIG, power factor control (or VAR control) and terminal voltage control will be carried out, considering different buses as reference during the investigation.

This paper is organized as follows. Section 2 provides an overview of the behavior of induction machines during transitory operation conditions. The applied dynamic models and their components are explained in Section 3. Section 4 presents the performed analysis of motor starting. In Section 5, the dynamic analysis during grid fault is discussed. Section 6 presents the main conclusions.

2. Dynamic behavior of induction machines

Voltage sags and interruptions produce each year in the United States a major economic damage estimated to be between U.S. $104 billion and U.S. $164 billion [16]. The voltage sags can be caused by short circuits at transmission and distribution levels, large load variations and IMs starting [1]. Voltage sags last from a few cycles to 1 min [4]. The shape of the voltage depends on network topology, line and cable impedances, load dynamic and the type of disturbance [4]. The induction motor is a source of disturbance (when is starting) and also an affected equipment (while in steady-state operation or also in starting process).

The dynamic behavior of the induction machine can be analyzed by the equivalent circuit of squirrel-cage induction machine presented in Fig. 1a, where R_S and R_R are the stator resistance and rotor resistance referred to the stator; X_S is the stator leakage reactance; X_R is the referred locked-rotor reactance; L_R is the referred rotor inductance; X_M is the magnetizing reactance; V_T is the terminal voltage per phase; s is the slip.

In order to analyze the electromagnetic torque, the circuit of Fig. 1a can be represented by its *Thévenin* equivalent circuit in Fig. 1b, where V_{TH}, R_{TH} and X_{TH} are the stator Thévenin circuit components, they are given by:

$$V_{TH} = V_{\phi}\frac{X_M}{\sqrt{R_S^2 + (X_S + X_M)^2}} \quad (1)$$

$$Z_{TH} = R_{TH} + jX_{TH} = \frac{jX_M(R_S + jX_S)}{R_S + j(X_S + X_M)} \quad (2)$$

The influence of voltages sags on the induction machine electromagnetic torque can be seen by analyzing its steady-state equations, see Eq. (3). Such equation shows the relation between the produced electromechanical torque and machine terminal voltage (in this case, the Thévenin voltage), adapted from the generator equations presented in Grilo et al. [17].

$$T_e = \frac{3V_{TH}^2\left(R_R/S\right)}{\omega\left[\left(R_{TH} + R_R/S\right)^2 + (X_{TH} + X_R)^2\right]} \quad (3)$$

where T_e is the electromagnetic torque; ω_{sync} is the synchronous angular velocity;

For motor operation, the largest value of X_R and V_{ab} (induced rotor voltage, see Fig. 1) occurs when the induction motor is at rest ($X_R = 2.\pi.f_S.L_R$) and the frequency of the induced voltage at the rotor (f_R) is equal to f_S (60 Hz for this case). The rotor reactance (X_R) and the induced rotor voltage decreases until the rotor achieves its nominal speed. At the nominal speed, the rotor frequency (f_R) depends on the rotor slip (s) and is equal to "$s.f_S$". The nominal slip (around 0.04) is very small compared to the slip at rest (equal to 1). This fact can explain the large amount of reactive power consumption during motor starting.

The quadratic relationship between electromagnetic torque and terminal voltage, shown in Eq. (3), indicates the negative impact of voltage sags. During a voltage sag, the electromagnetic torque will decrease, resulting in decrease (for motors) or increase (for generators) of the rotor speed. As a result, the machine will require more reactive power from the grid. To sum up, the consumption of reactive power by the motor increases when starting or recovering its nominal speed and, by consequence, the depth of the voltage sag and its duration [1].

There are several methods to avoid high voltage sags during IM starting. The most adequate starting method depends on the power system constraints and characteristics, the load to be accelerated and the overall costs of the additional equipment [7]. The main methods are: (a) The full voltage method (or direct connection): It is the cheapest and most commonly employed method. The implementation produces high starting torque, the highest required reactive current and the shortest acceleration time [7]. (b) Reduced Voltage Starting Methods: A reduced voltage is applied and it returns to the nominal value when a predefined speed (or current) set-point is reached [7]. The control of the voltage can be performed by solid-state starters, adjustable frequency drives, autotransformers, soft starter, external rotor resistances, wye-delta connection changes and changes in windings connection types.

Since the voltage sag can be reflected at buses in the vicinity, not only the voltage behavior at the local buses should be verified. The choice of the starting method should also consider other components of the system, for instance, distributed generators connected to the same system. As already pointed out, induction generator-based wind turbines are usually provided with power electronic-based equipment that can be employed for voltage support during disturbances in the grid. These resources can be used to minimize the impact of starting a large motor in the grid or even minimize the duration of voltage sags after faults in the system.

Please cite this article in press as: M.A. Paez, et al., Voltage support in industrial distribution systems in presence of induction generator-based wind turbines and large motors, Electr. Power Syst. Res. (2016), http://dx.doi.org/10.1016/j.epsr.2016.05.001

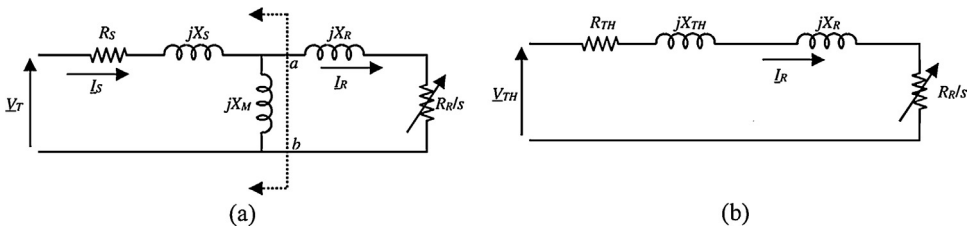

Fig. 1. Steady-state equivalent circuit of an induction machine. (a) Complete circuit. (b) Thévenin equivalent circuit.

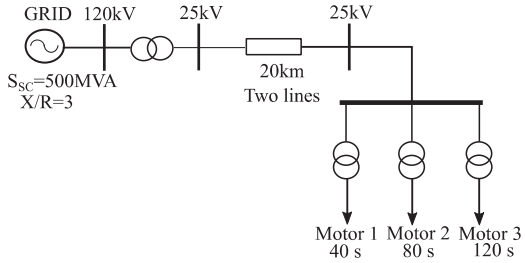

Fig. 2. Test power system configuration with swing bus only.

3. Computational dynamic models

The software used in the phasor simulation mode is a Matlab/Simulink toolbox called SymPowerSystem. This toolbox has already implemented many electrical components of power systems, however, adaptations of existing models and new models were built. More information, as and the sets and parameters of the simulation electrical components, can be found below.

3.1. The test system

The system used in the simulations is illustrated in Fig. 2. It comprises an industrial power distribution system connected to a transmission system by a double circuit line of 20 km length. The transmission system is represented by an infinite bus at a voltage level of 120 kV. Three identical industrial plants are connected to the distribution system via three transformers, each one of 2.5 MVA (2.3 kV/25 kV). Each plant includes one 200 kW resistive load (such as space heaters and a 5% parasite load required by SimPowerSystem to connect motors in series with transformers) and a large IM load (1,68 MW at 0,93 PF). The representation in Fig. 2 of each Motor load includes the IM itself and the parallel resistive load for simplicity.

3.2. Squirrel-cage induction motors

The dynamic model available in SimPowerSystem is used with a modification of the mechanical torque (*Tm*) applied to the motors. The mechanical torque is implemented in per-unit and is proportional to the square of rotor angular speed ($0.9\,\omega_m{}^2$), as usual for representing pump and fan loads. The electrical model is a fifth-order model in *dq0* axis reference frame (three stator and two rotor differential voltage equations). The motor parameters can be found in Table 1.

3.3. Squirrel cage induction generator-based wind turbine model

In this configuration, the stator windings are connected directly to the grid in 60 Hz (or 50 Hz), see Fig. 3. The speed operation of the rotor is very narrow slip variation [7,15,17]. The rotor blades are equipped with variable−pitch angle mechanism.

Small wind farms can be represented with accuracy by an aggregated model because the speed of the wind that arrives in each wind turbine can be considered the same, as suggested in García et al. [18]. The aggregated wind turbine has 9 MW of rated power, representing six wind turbines of 1.5 MW each. The implemented model already exists in SimPowerSystems without the capacitor bank. The phasor model of the generator is based on the induction motor model, presented in Section 3.2. The mechanical model is based on the well-known equation for extraction of power from the wind [11] and includes a pitch angle control (limits the electrical power to the rated value). The SCIG parameters can be found in Table 2.

Table 1
Squirrel-cage induction motors parameters.

Parameter	Value	Parameter	Value
Nominal Power	1.8 MVA	R_s	0.0092 p.u.
Line-To-Line Voltage	2300 V	L_{ls}	0.0717 p.u.
Frequency	60 Hz	R_r	0.0070 p.u.
H	0.5 s	L_{lr}	0.0717 p.u.
Pair of pole	2	L_m	4.14 p.u.

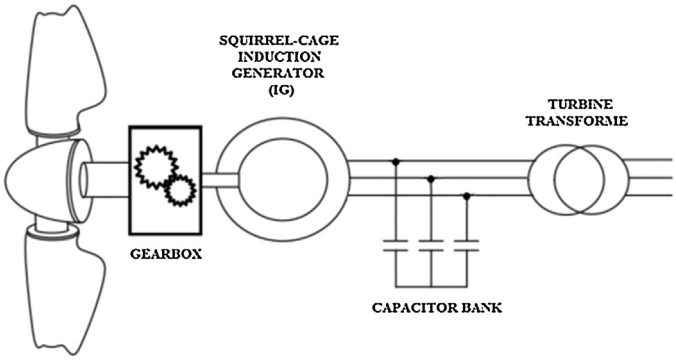

Fig. 3. Configuration of a SCIG-based wind turbine.

Table 2
Squirrel-cage induction generators.

Parameter	Value	Parameter	Value
Nominal Power	1.66 MVA	R_s	0.004843 p.u.
Line-To-Line Voltage	575 V	L_{ls}	0.1248 p.u.
Frequency	60 Hz	R_r	0.004377 p.u.
Inertia constant	5.04 s	L_{lr}	0.1791 p.u.
Friction factor	0.01 p.u.	L_m	6.77 p.u.
Pairs of poles	3		

3.4. Doubly-fed induction generator model

The doubly-fed induction generator (DFIG) has the rotor windings connected to the grid through a back-to-back converter. The stator windings are connected directly to the grid in 60 Hz (or 50 Hz). A typical configuration of a DFIG wind turbine is shown in Fig. 4, more details can be found in [8,11,15].

The aggregation model can also be used for the DFIG-based wind turbine. The mechanical model of the turbine is equal to the one

Please cite this article in press as: M.A. Paez, et al., Voltage support in industrial distribution systems in presence of induction generator-based wind turbines and large motors, Electr. Power Syst. Res. (2016), http://dx.doi.org/10.1016/j.epsr.2016.05.001

Table 3
Doubly-fed induction generators.

Parameter	Value	Parameter	Value
Nominal Power	1.66 MVA	R_s	0.0071 p.u.
Line-To-Line Voltage	575 V	L_{ls}	0.1710 p.u.
Frequency	60 Hz	R_r	0.0050 p.u.
Inertia constant	5.04 s	L_{lr}	0.1560 p.u.
Friction factor	0.0100 p.u.	L_m	2.9000 p.u.
Pairs of poles	3	Grid-side coupling resistance	0.0015 p.u.
Converter maximum power	0.5	Nominal DC bus voltage	1200 V
Grid-side coupling inductor	0.1500 p.u.		

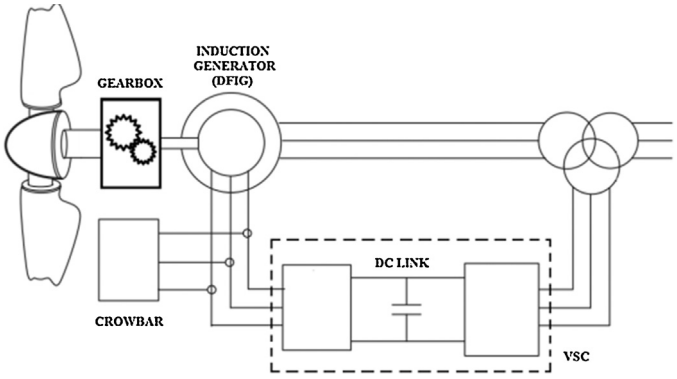

Fig. 4. Schematic configuration of a DFIG-based wind turbine.

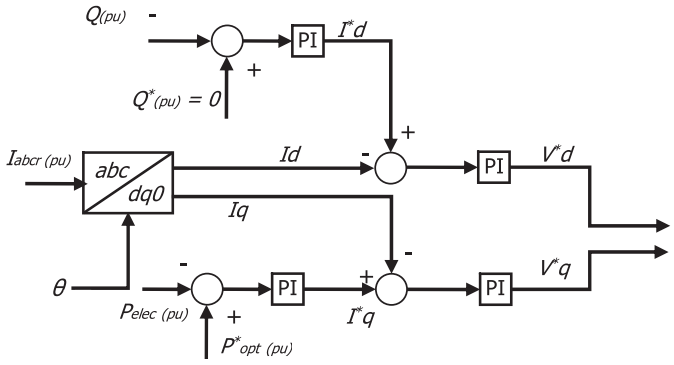

Fig. 5. RSC of a DFIG-based wind turbine.

presented in Section 3.2, including the pitch angle mechanism. The electrical machine model is very similar to the induction machine presented in Section 3.2, however, it has an extra term for the external applied rotor voltage in *dq* axis reference frame, as presented in Salles et al. [11]. The DFIG-based wind turbine parameters can be found in Table 3.

3.5. Controller models of DFIG

The implemented models already exist within SimPowerSystems, however an adaption has been made for the case in which the reactive power control is performed in addition by the grid side converter (GSC). The original controller enables only the reactive power injection by the rotor side converter (RSC).

The rotor mechanical speed is decoupled from the grid frequency and can enable variable speed operation. The typical range for the rotor speed is ±30% of synchronous speed. The rotor side converter (RSC) controls the rotor speed to follow the Maximum Power Point Tracking (MPPT), shown in Fig. 5 by the optimal power (P^*_{opt}). The RSC is also responsible for the reactive power control of the DFIG [11]. The reactive power can be controlled for unitary

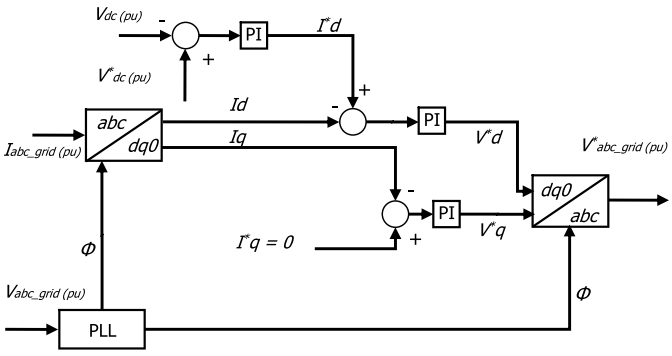

Fig. 6. GSC of a DFIG-based wind turbine controlling the DC-link voltage.

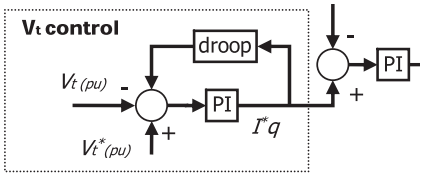

Fig. 7. GSC control modification to enable reactive power injection.

power factor using zero reactive power injection reference $Q^* = 0$ (Fig. 5). Different reference values, such as the terminal voltage, can be implemented replacing Q^* by $V_T{}^*$ and the measured signal Q by V_T.

The conventional operation of the grid side converter (GSC) is to maintain the voltage at the DC-link in a reference value [8,11,15]. In Fig. 6, the schematic GSC control is presented. The DC-link voltage can be controlled by comparing its reference voltage $V_{dc}{}^*$ to the measured V_{dc} and send to a PI block. The reference current in the direct axis (I^*_d) will be compared to the measured related current and will be sent to the second level of PI controller. The direct and the quadrature axis reference voltages will be converted to the *abc* model and will be applied to the grid.

The modification included in the model is presented in Fig. 7. This additional block replaces the current reference signal I^*_q in Fig. 6, comparing the terminal voltage as reference signal and enabling the injection of reactive power by the GSC. The use of a droop sets an action delay to the control, no swinging interaction with the RSC control was observed in the simulations. For high values of Kp (the proportional gain parameter of the PI controller), the reference current I^*_q works as an on-off system, applying the rated reactive current value to the grid side converter.

Many control strategies have been proposed in the literature, mainly against short-circuits and voltage sags in transmission systems [8,19]. The performed analysis in this paper for GSC control strategy presented in Fig. 7 has not yet been proposed for industrial power distribution systems.

Please cite this article in press as: M.A. Paez, et al., Voltage support in industrial distribution systems in presence of induction generator-based wind turbines and large motors, Electr. Power Syst. Res. (2016), http://dx.doi.org/10.1016/j.epsr.2016.05.001

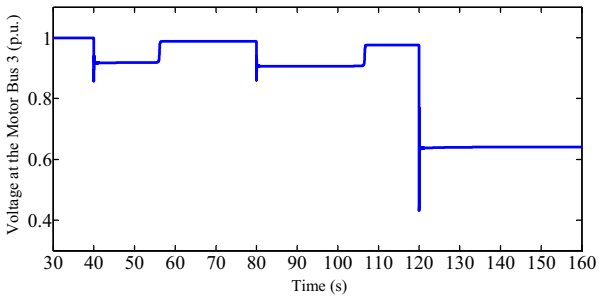

Fig. 8. Terminal voltage at motor 3 during sequential direct connection.

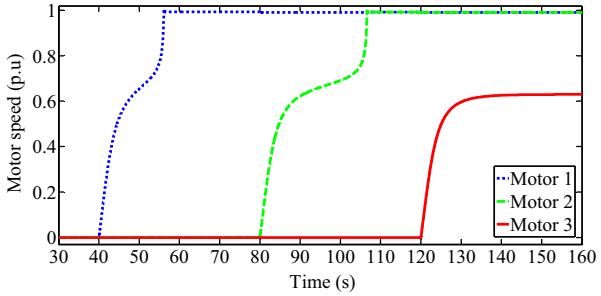

Fig. 9. Motor speed during sequential direct connection.

4. Simulation of large motor starting

As described in Section 3, there are a few methods to start motors. When large motors start in sequence using the direct connection method, the grid voltage may be affected. The worse scenario may happen when the grid is the only power source supplying the motor reactive power needs. We have performed the analysis on "motor 3" terminal voltage during the motor starting sequence (Fig. 8). The sequence of starting is: motor 1 at 40 s, then motor 2 at 80 s and motor 3 at 120 s (from Fig. 2 test system). After motor 1 and 2 reached the full speed, the terminal voltages did not recover the pre-starting value, however, the voltages are still inside the limits.

Because of the lack of reactive power at the distribution system, motor 3 did not have enough electromagnetic torque to achieve full speed, as can be seen in Fig. 9. Motor 1 and 2 developed full speed after 17 and 27 s, respectively.

This sequence of IM starting is used as base case for analyzing the system behavior with a small wind farm, employing either SCIG or DFIG. These generators are provided with voltage support equipment based on the existing technology and on possible advanced configurations that may need small changes in control algorithm only. The analyzed cases are summarized as follow: (A) SCIG-based wind farm: 1) capacitor bank; 2) STATCOM; 3) soft starter and STATCOM. (B) DFIG-based wind farm: 1) unitary power factor control; 2) terminal voltage control; 3) terminal voltage at motor 3; 4) terminal voltage control (GSC and RSC).

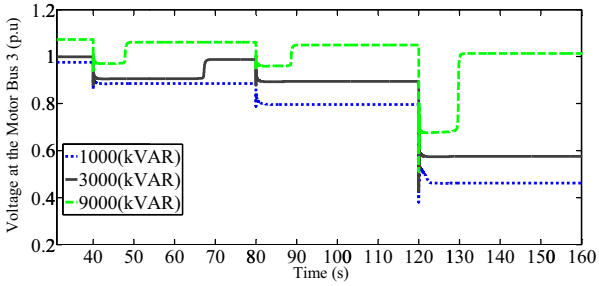

Fig. 11. Terminal voltage at motor 3 during sequential motor starting (Capacitor Bank).

4.1. SCIG-based wind farm (Case A)

4.1.1. SCIG with capacitor bank (A-1)

The use of capacitor banks provides reactive power to the SCIG's and improves its power factor [7,11]. The rated power of the capacitor banks is usually around 30% of the wind farm installed capacity, different capacitor banks rated power are analyzed. The test system is presented in Fig. 10.

The terminal voltage at motor 3 for different rated power of the capacitors bank is shown in Fig. 11. One can see that with high reactive power compensation (9 MVAr in this case), the grid voltage achieves higher level and the motor 3 is able to reach full speed. The capacitor banks reduce the required reactive power from the system (which is not only required by the motors but by the SCIG-based wind farm).

The capacitor banks should be used carefully to avoid overvoltage during normal operation and also to avoid the operation of the large motors as generators due its inertial energy in acceleration. The capacitor bank of the wind farm may be limited to 1/3 of its rated power.

4.1.2. Static synchronous compensator–STATCOM (A-2)

The use of STATCOM-based on power electronic (such as IGBTs, IGCTs, or GTOs) enables the wind farm to supply or absorb reactive power with fast response at reduced voltage levels [8]. From personal communication with a member of the S&C Electric Company, one of the greatest markets for STATCOMs is the wind farms in distributed systems of the United Kingdom, in order to accomplish with the grid codes. The test system used is the same presented in Fig. 10, replacing the capacitor bank by the STATCOM. The voltage profiles for the motor starting sequence are presented in Fig. 12 for three different STATCOM power. As one can see, the results are very similar to those obtained when considering a capacitor bank, it is seen that the voltage doesn't exceed the reference value of 1 p.u.

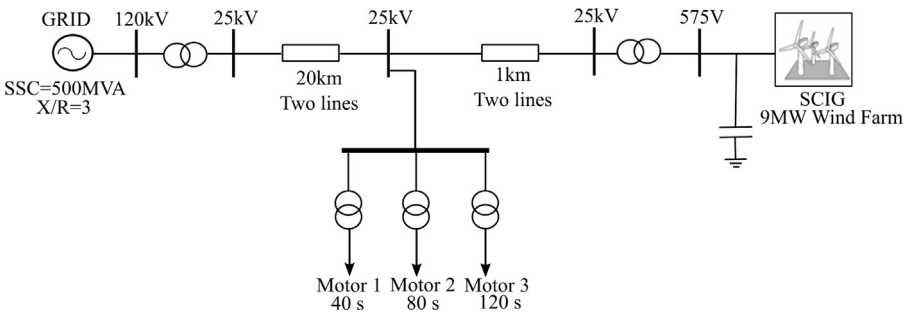

Fig. 10. Schematic diagram of the test system with SCIG and capacitor bank.

Please cite this article in press as: M.A. Paez, et al., Voltage support in industrial distribution systems in presence of induction generator-based wind turbines and large motors, Electr. Power Syst. Res. (2016), http://dx.doi.org/10.1016/j.epsr.2016.05.001

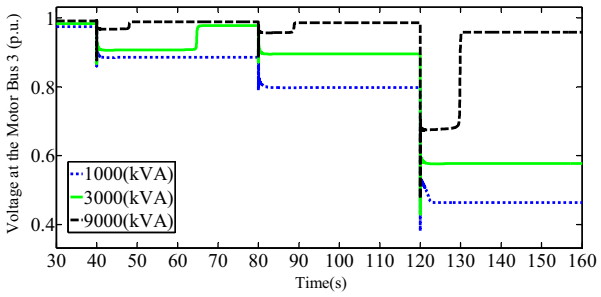

Fig. 12. Terminal voltage during a sequential motor starting (STATCOM).

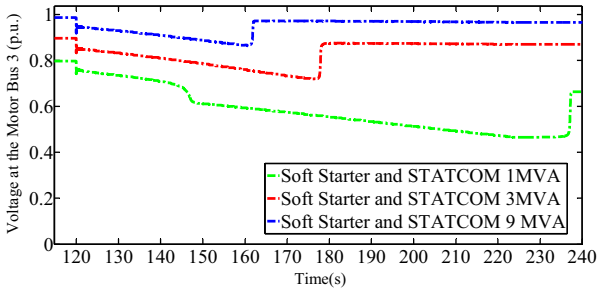

Fig. 13. Terminal voltage at motor 3 with soft starter and STATCOM.

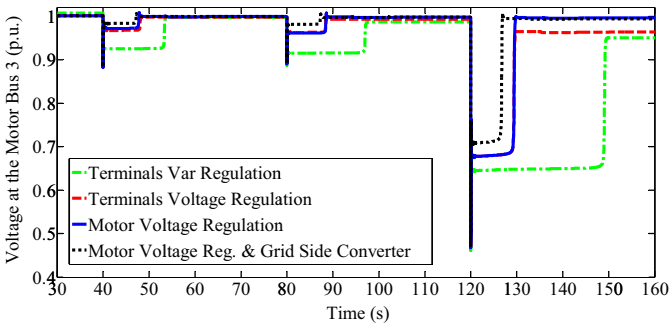

Fig. 15. Terminal voltage at the motor 3 with DFIG.

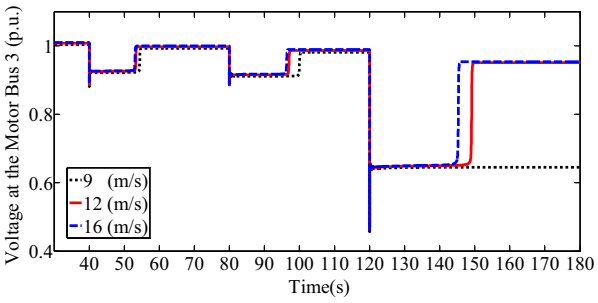

Fig. 16. Voltage at motor 3 terminals (DFIG - Terminals Var. Regulation).

4.1.3. Soft starter and STATCOM (A-3)

A basic soft starter model is connected at the terminal of motor 3. The soft starter has two main components: pulse generator and three-phase two-winding transformer with on-load tap changer (OLTC). The pulse generator acts as a controller, which applies a signal with 0 or 1 value to move the tap position upward or downward, respectively. The soft starter parameters are shown in Table 4. The relation between *Tm* and motor speed has been changed in motor 3 ($Tm = 0.9\,\omega_m{}^2$).

The terminal voltage is presented in Fig. 13 for the wind farm with STATCOM and the motor 3 with soft starter. It can be seen that the use of a soft starter decreases the voltage sags and reduces the reactive power required from the system during the starting. However, the required time to achieve rated speed is extended. The motor 3 operation still makes the terminal voltage below the limits, for rated capacity equal to 1 MVA. This solution attenuates the problem and could be an alternative for existing systems.

4.2. DFIG-based wind farm (Case B)

Wind farms based on DFIG have the possibility to inject or consume reactive power controlling the back-to-back converters. Fig. 14 shows the test power system used to study the behavior of DFIG. We have analyzed three control methods for the rotor side converter (RSC) and one with additional reactive power support from the grid side converter (GSC).

One can see from Fig. 15 that the system has the lowest recovery time when the control strategy "Motor Voltage regulation & GSC" is chosen. The control strategy "Terminals Var. Regulation" (unitary power factor control) represents the worst case. The system has the highest recovery time and reaches the lowest voltage. The voltage at the motor terminals is closer to 1 p.u. in steady-state for "Motor Voltage regulation". This result is better than the cases with the control strategies "Terminals Var. Regulation" and "Terminals Voltage Regulation".

4.3. DFIG-based wind farm and wind speeds

The control strategies of the DFIG-based wind farm for "Terminals Voltage Regulation" and "Terminals Var. Regulation" are analyzed during different incoming wind speeds. For low wind speed values, the "Terminals Var. Regulation" control mode behaviors like the motor starting with direct connection. The RSC is controlled to make the machine operate at unitary power factor. In such condition, motor 3 does not have the necessary starting torque to run to its nominal speed (Fig. 16).

The wind farm based on DFIG in "Terminal Voltage Regulation" mode keeps the voltage in tolerable levels providing the necessary

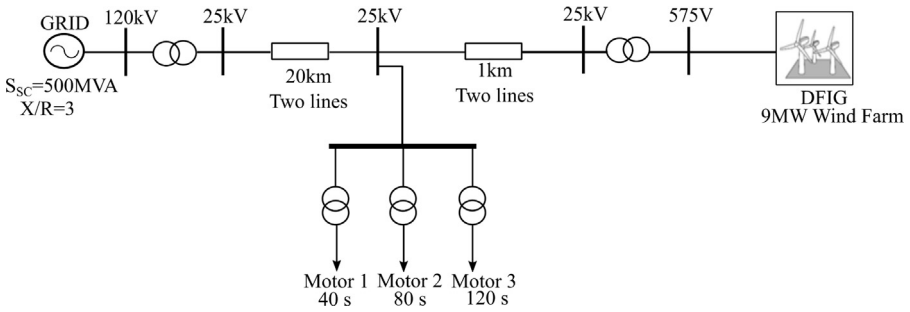

Fig. 14. Test power system configuration with DFIG.

Table 4
Soft starter parameters.

Parameter	Description	Parameter	Description
Voltage ratio	2300/2300V	OLTC minimum tap positions	−100
OLTC on	Winding 2	OLTC maximum tap positions	0
Time per tap	1.5 s	Initial tap position	−70
Voltage step delta Per tap (p.u.)	0.01	Final tap position	0

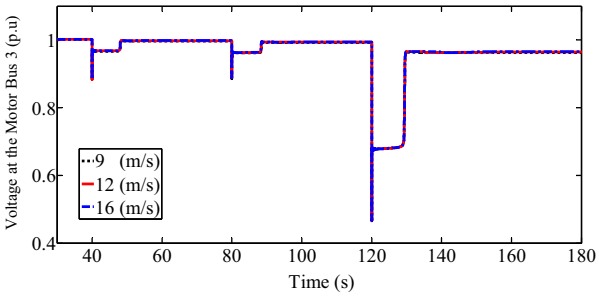

Fig. 17. Voltage at the motor 3 terminals (DFIG - Terminals Voltage Regulation).

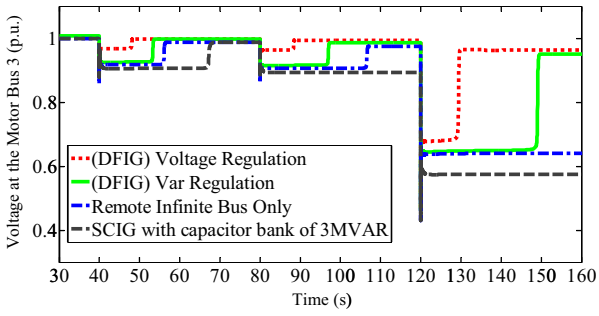

Fig. 18. Voltage at the motor 3 bus (motor starting).

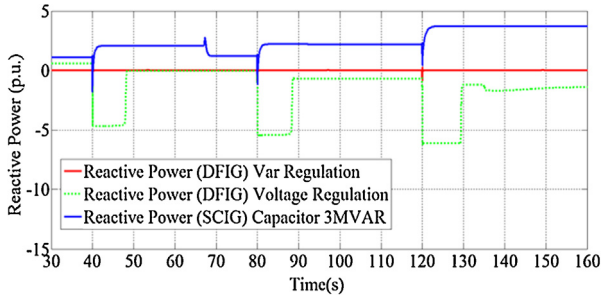

Fig. 19. Reactive power exchanged at the wind farm bus.

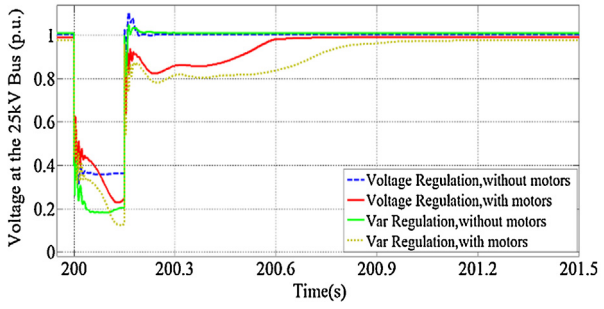

Fig. 20. Voltage at the 25 kV bus during grid fault.

reactive power to a successful motor 3 starting, as can be seen in Fig. 17.

The above simulations show that wind farm based on DFIG with Terminal Voltage regulation control increases the stability margin of the system providing more reactive power compared to Var Regulation control for different wind speeds.

4.4. Considerations about motor starting in systems with wind farms

The voltage at the connection point of motor 3 is summarized in Fig. 18. The DFIG converters provide an advantage compared to conventional SCIG regarding to the generation or absorption of reactive power. The DFIG-based wind farm in "Terminals Voltage Regulation" and in "Terminals Var. Regulation" modes have better performance during the motor starting (Fig. 18).

The lowest recovery time is observed when the "Terminals Voltage Regulation" is in use, the voltage profile doesn't exceed the up reference value of 1 p.u. In this control mode, the DFIG absorbs reactive power before the motor starting at $t = 40$ s (Fig. 19), maintaining the grid voltage at 1 p.u. The scenario based on SCIG only consumes reactive power from the grid and cannot recover the voltage, it could lead the system to an unstable operation region.

5. Industrial plants and wind farms during grid faults

Low voltage ride through (LVRT) capability of wind farms defines its ability to continue uninterrupted operation during voltage sags [20,21]. When the surrounding network has large induction motors, the behavior during grid faults might be affected negatively. When steady-state operation of the system is achieved (for any succeeding process described above), all the three industrial plants will be operating at full load and motors will be running at the nominal speed. The test system showed in Fig. 14 is used to analyze the behavior of the DFIG during grid fault in the presence of large motors.

The model of DFIG-based wind turbine during grid faults may be different from the model considering voltage sags only, a protective converter scheme [22] and uninterrupted power control [23] might be added. The crowbar system is an essential hardware to protect the RSC from overcurrents induced in the rotor windings, different topologies are proposed in the literature [24]. The DC-chopper is also an important protective hardware to guarantee the voltage limits of the DC-link [25]. The reactive power injection can also be achieved using special control techniques during and after the fault [26]. The adopted model for the simulation presented in this paper does not consider this two protective scheme (crowbar and DC-chopper) and the control mode of the DFIG does not change during the simulation. However, these simplifications do not compromise the comparative results.

The voltage at the Point of Common Coupling (PCC) of the DFIG-based wind farm (25 kV bus) during a three-phase fault at the 120 kV bus is shown in Fig. 20. The voltage sags analyzed for two DFIG control scheme ("Terminals Voltage Regulation" and "Terminals Var. Regulation"). Fig. 20 shows that the voltage magnitude drops in all cases at the beginning of the fault (time = 200s). For the case that the three motors are in operation, there is a deeper decay in the voltage. When the fault is cleared, all motors attempt to re-establish their internal voltage and reaccelerate. This process makes them absorbs a large amount of reactive power from the

Please cite this article in press as: M.A. Paez, et al., Voltage support in industrial distribution systems in presence of induction generator-based wind turbines and large motors, Electr. Power Syst. Res. (2016), http://dx.doi.org/10.1016/j.epsr.2016.05.001

system. By consequence, the terminal voltage has a second sag during the motor reacceleration. This behavior differs from the conventional rectangular phenomenon [4].

The characteristic of the voltage sag during the fault depends on the required mechanical load of the motor. Motors with constant mechanical load have higher speed variations during voltage sag compared to motors coupled with speed-squared torque. Thus, motors with constant mechanical load have greater recovery time [7].

One can conclude from the simulation results presented in Fig. 20 that the DFIG-based wind farm with a control strategy that regulates the terminal voltage presents better performance during the fault period recovering the steady-state values. The coordination with the industrial power plant equipped with large motors would be a better and cheaper solution, since there is no need of extra wind turbine hardware, the adaptations would be performed only inside the control algorithm.

6. Conclusions

This paper has analyzed the impact of large induction motors on the dynamic performance of distribution networks in the presence of a wind farm. The study is restricted to wind farms with small installed capacity compared to the local industrial plants. The results show that the technology of the wind generators and the applied control scheme have a significant influence on system stability and on the voltage recovery time.

Is has been seen that even a critical wind farm technology, using squirrel cage induction generator, with the appropriate reactive power resource can improve the voltage at the power system during the starting of large motors. It has also been verified that DFIGs controlling motor terminal voltage and injecting reactive power through the grid side converter can improve system stability during the connection of large induction motors.

During grid faults, the operation of large induction motors can affect the voltage sag shape differently from the conventional rectangular sag phenomenon. In such events, the DFIGs terminal voltage control can be used to provide the required reactive power by the motors reacceleration period, helping the voltage recovery. Although this control mode is not yet available in modern wind turbines, it could be easily set using the actual resources available in a typical DFIG. Such control could be very useful for weak power systems.

As a result, it is possible to take advantage of the available voltage support resources not only for improving voltage ride through capability of DFIG-based wind farms, but also to improve the system power quality levels during voltage sags caused by starting motors and faults in the system.

Acknowledgment

The authors gratefully acknowledge the financial support from Brazil by São Paulo Research Foundation FAPESP (grant # 2012/09989-2 and grant # 2010/20250-3) and National Counsel of Technological and Scientific Development CNPq to this research.

References

[1] X. Wang, J. Yong, W. Xu, W. Freitas, Practical power quality charts for motor starting assessment, IEEE Trans. Power Deliver. 26 (April (2)) (2011).
[2] M. Falahi, K.L. Butler-Purry, M. Ehsani, Induction motor starting in islanded microgrids, IEEE Trans. Smart Grid 4 (September (3)) (2013) 1323–1331.
[3] A. Polycarpou, H. Nouri, Validation of a proposed voltage sag prediction methodology for interconnected systems during motor starting, in: Proc. 44th Int. Universities Power Engineering Conf., Glasgow, pp. 1–5,UK, 2009.
[4] P. Aree, Effects of large induction motors on voltage sage, in: Power and Energy Engineering Conference (APPEEC), 2012 Asia-Pacific, pp.1-4, 27-29 March, 2012.
[5] IEEE, Recommended practice for industrial and commercial power systems analysis, IEEE Std. 399 (1997).
[6] IEEE Recommended Practice for Electric Power Distribution for Industrial Plants, IEEE Std 141-1993.
[7] W. Freitas, J.C.M. Vieira, A. Morelato, L.C. Da Silva, P. Da Costa, V.F. Lemos, A.B. Flavio, Comparative analysis between synchronous and induction machines for distributed generation applications, IEEE Trans. Power Syst. 21 (February (1)) (2006) 301–311.
[8] R. Cardenas, R. Pena, S. Alepuz, G. Asher, Overview of control systems for the operation of DFIGs in wind energy applications, IEEE Trans. Ind. Electron. 60 (July (7)) (2013) 2776–2798.
[9] Y. Liao, H. Li, J. Yao, K. Zhuang, Operation and control of a grid-connected DFIG-based wind turbine with series grid-side converter during network unbalance, Electr. Power Syst. Res. 81 (January (1)) (2011) 228–236.
[10] A.H.M.A. Rahim, I.O. Habiballah, DFIG rotor voltage control for system dynamic performance enhancement, Electr. Power Syst. Res. 81 (February (2)) (2011) 503–509.
[11] M.B.C. Salles, J.R. Cardoso, A.P. Grilo, C. Rahmann, K. Hameyer, Control strategies of doubly fed induction generators to support grid voltage, in: IEEE International Electric Machines and Drives Conf. (IEMDC '09), pp.1551-1556, 3-6 May, 2009.
[12] R. Londero, C. De Mattos Affonso, J.P. Abreu Vieira, Long-term voltage stability analysis of variable speed wind generators, IEEE Trans. Power Syst. 30 (January (1)) (2015) 439–447.
[13] B. Kanoj, M. Arjun Sanu, A.B. Raju, Steady state analysis of autonomous wind energy conversion system for irrigation purpose employing induction machines using python-a free and open source software, in: Global Humanitarian Technology Conference: South Asia Satellite (GHTC-SAS), 2013, pp. 292–297.
[14] J. Xu, S. Liao, Y. Sun, X. Ma, W. Gao, X. Li, J. Dong, An isolated power systems driven by wind-coal power for aluminum productions: A case study of frequency control, IEEE Trans. Power Syst. 30 (1) (2015) 471–483.
[15] H. Polinder, J.A. Ferreira, B.B. Jensen, A.B. Abrahamsen, K. Atallah, R.A. McMahon, Trends in wind turbine generator systems, IEEE J. Emerg. Selected Topics Power Electron. 1 (September (3)) (2013) 174–185.
[16] O. Ipinnimo, S. Chowdhury, S.P. Chowdhury, J. Mitra, Intelligent voltage dip detection in power networks with distributed generation (DG), in: North American Power Symposium (NAPS), 2012, September, p. pp.1-6.
[17] A.P. Grilo, A.d.A. Mota, L.T.M. Mota, W. Freitas, An analytical method for analysis of large-disturbance stability of induction generators, IEEE Trans. Power Syst. 22 (November (4)) (2007) 1861–1869.
[18] C.A. García, L.M. Fernández, F. Jurado, Evaluating reduced models of aggregated different doubly fed induction generator wind turbines for transient stabilities studies, Wind Energy 18 (1) (2015) 133–152.
[19] M. Tazil, V. Kumar, R.C. Bansal, S. Kong, Z.Y. Dong, W. Freitas, H.D. Mathur, Three-phase doubly fed induction generators: an overview, Electr. Power Appl. IET 4 (February (2)) (2010) 75–89.
[20] M. Tsili, S. Papathanassiou, A review of grid code technical requirements for wind farms, Renew. Power Gener. IET 3 (September (3)) (2009) 308–332.
[21] M. Mohseni, S.M. Islam, Review of international grid codes for wind power integration: Diversity technology and a case for global standard, Renew. Sust. Energ. Rev. 16 (6) (2012) 3876–3890.
[22] K.E. Okedu, S.M. Muyeen, R. Takahashi, J. Tamura, Wind farms fault ride through using DFIG with new protection scheme", IEEE Trans. Sust. Energ. 3 (April (2)) (2012) 242–254.
[23] D.F. Howard, L. Jiaqi, R.G. Harley, Short-circuit modeling of DFIGs with uninterrupted control, IEEE J. Emerg. Sel. Top. Power Electron. 2 (March (1)) (2014) 47–57.
[24] J. Vidal, G. Abad, J. Arza, S. Aurtenechea, Single-phase DC crowbar topologies for low voltage ride through fulfillment of high-power doubly fed induction generator-based wind turbines, IEEE Trans. Energ. Conver. 28 (September (3)) (2013) 768–781.
[25] G. Pannell, B. Zahawi, D.J. Atkinson, P. Missailidis, Evaluation of the performance of a DC-link brake chopper as a DFIG low-voltage fault-ride-through device, IEEE Trans. Energ. Conver. 28 (September (3)) (2013) 535–542.
[26] D. Xie, Z. Xu, L. Yang, J. Ostergaard, Y. Xue, K.P. Wong, A comprehensive LVRT control strategy for DFIG wind turbines with enhanced reactive power support, IEEE Trans. Power Syst. 28 (August (3)) (2013) 3302–3310.

Please cite this article in press as: M.A. Paez, et al., Voltage support in industrial distribution systems in presence of induction generator-based wind turbines and large motors, Electr. Power Syst. Res. (2016), http://dx.doi.org/10.1016/j.epsr.2016.05.001